J Fluoresc (2013) 23:649–657
DOI 10.1007/s10895-013-1175-0

ORIGINAL PAPER

A Novel Homogeneous Time-Resolved Fluoroimmunoassay for Carcinoembryonic Antigen Based on Water-Soluble Quantum Dots

Zhen-Hua Chen · Ying-Song Wu · Mei-Jun Chen · Jing-Yuan Hou · Zhi-Qi Ren · Da Sun · Tian-Cai Liu

Received: 26 December 2012 / Accepted: 24 February 2013 / Published online: 8 March 2013

Abstract Quantum dots are not widely used in clinical diagnosis. However, the homogeneous time-resolved fluorescence assay possesses many advantages over current methods for the detection of carcinoembryonic antigen (CEA), a primary marker for many cancers and diseases. Therefore, a novel luminescent terbium chelates- (LTCs) and quantum dots-based homogeneous time-resolved fluorescence assay was developed to detect CEA. Glutathione-capped quantum dots (QDs) were prepared from oil-soluble QDs with a 565 nm emission peak. Conjugates (QDs-6 F11) were prepared with QDs and anti-CEA monoclonal antibody. LTCs were prepared and conjugates (LTCs-S001) were prepared with another anti-CEA monoclonal antibody. The fluorescence lifetime of QDs was optimized for sequential analysis. The Förster distance (R_0) was calculated as 61.9 Å based on the overlap of the spectra of QDs-6 F11 and LTCs-S001. Using a double-antibody sandwich approach, the above antibody conjugates were used as energy acceptor and donor, respectively. The signals from QDs were collected in time-resolved mode and analyzed for the detection of CEA. The results show that the QDs were suitable for time-resolved fluoroassays. The spatial distance of the donor-acceptor pair was calculated to be 61.9 Å. The signals from QDs were proportional to CEA concentration. The standard curve was LogY=2.75566+0.94457 LogX (R=0.998) using the fluorescence counts (Y) of QDs and the concentrations of CEA (X). The calculated sensitivity was 0.4 ng/mL. The results indicate that water-soluble QDs are suitable for the homogenous immunoassay. This work has expanded future applications of QDs in homogeneous clinical bioassays. Furthermore, a QDs-based homogeneous multiplex immunoassay will be investigated as a biomarker for infectious diseases in future research.

Keywords Water-soluble quantum dots · Homogeneous immunoassay · FRET · Terbium chelates · Carcinoembryonic antigen

List of Abbreviations

6 F11	Anti-CEA monoclonal antibody
AFP	Alpha-fetoprotein
BS3	Bis(sulfosuccinimidyl) suberate sodium salt
CEA	Carcinoembryonic antigen
cs124	7-amino-4-methyl-2(1H)-quinolinone
DMSO	Anhydrous dimethyl sulfoxide
DTPA	Diethylene triamine pentacetic acid
DTPAa	Diethylenetriaminepentaacetic acid dianhydride
EDA	Ethylenediamine
EDAC	(N-(3-dimethyllaminopropyl) carbodiimide hydrochloride
EDTA	Ethylenediaminetetraacetic acid
FRET	Förster resonance energy transfer
FWHM	Full-width at half maximum
GSH	Glutathione reduced
HTRFAs	Homogeneous time-resolved fluoroassays
LTCs	Luminescent terbium chelates
McAb	Monoclonal antibody
MES	2-[N-morpholino]ethanesulfonic acid

Zhen-Hua Chen and Ying-Song Wu contributed equally to this work

Z.-H. Chen · Y.-S. Wu · M.-J. Chen · J.-Y. Hou · Z.-Q. Ren · D. Sun · T.-C. Liu (✉)
School of Biotechnology, Southern Medical University, Guangzhou 510515, Guangdong, People's Republic of China
e-mail: liutc@smu.edu.cn

oQDs	Oil-soluble quantum dots
PBS	Phosphate buffered saline
QDs	Quantum dots
QY	Quantum yield
S001	Anti-CEA monoclonal antibody
SD	Standard deviation
sulfo-NHS	N-hydroxysulfosuccinimide sodium salt
TOPO	Tri-n-octylphosphine oxide
TR-FRET	Time-resolved Förster resonance transfer
Tris	Tris(hydroxymethyl)aminomethane
wQDs	Water-soluble quantum dots

Introduction

Carcinoembryonic antigen (CEA) is a non-organ-specific, tumor-associated antigen, which is a glycoprotein of molecular mass approximately 200 kDa. It was first described as a specific indicator of colorectal carcinoma by Gold and Freedman in 1965 [1, 2]. CEA has become one of the most common tumor markers and is reliable for clinical diagnosis of colorectal [3], pancreatic [4], gastric [5], and cervical carcinomas [6]. In healthy individuals, the serum CEA level is at an upper limit of 2.5 $ngmL^{-1}$ [7, 8]. Patients with gastrointestinal cancer have a higher concentration of CEA in serum compared with healthy individuals [9]. In addition, a high level of CEA in serum is related to breast cancer [10], lung cancer [11, 12], cystadenocarcinoma [13] and other malignancies [14, 15]. Similarly, raised CEA concentrations have been detected in cigarette smokers [16, 17]. Therefore, the determination of the serum CEA level is very important in the diagnosis of malignant tumors, treatment evaluation and disease surveillance during therapy.

During the past few decades, a number of analytical methods for human CEA have been described, including the enzyme-linked immunosorbent assay [18], radioimmunoassay[19, 20], time-resolved fluoroimmunoassay[21–23], chemiluminescence immunoassay [24, 25] and chemiluminescent enzyme immunoassay [26, 27].

All of the above methods are heterogeneous assays, where CEA is coated onto a plate and unlabeled species must be washed away. Most are time-consuming, isotope-radioactive or have low sensitivity. They also suffer low signal-noise ratios when traditional fluorescent labels are used because of autofluorescence from the light source. Time-resolved fluorometry of lanthanide chelates has been shown to be one of the most successful non-isotopic detection techniques and it is therefore employed in numerous applications in the biomedical sciences [28–30]. However, the antigen or antibody is usually immobilized on the surface of a 96-well microplate by physical absorption, so it is unstable and can easily be washed away.

Furthermore, the prognosis for advanced cancers remains poor and new treatments and more advanced diagnosis strategies are urgently needed. A recent trend has been to develop homogeneous time-resolved fluoroassays (HTRFAs) to save time and enhance signal-noise, based on Förster resonance energy transfer (FRET). This approach is taken because in time-resolved mode, the ratio of positive signal to noise is magnified many times without interference from noise caused mainly by the excitation light resource and auto-fluorescence of the background. This approach could offer a significant advantage over the traditional homogeneous fluoroassay (without time-resolved fluorescence), namely that excess labeling need not be washed away during the investigation of molecular events [31–34]. Potentially, the protocols involved would be valid, novel, and much more convenient and easily automated than the traditional homogenous fluoroassay once suitable commercial reagents are available.

Fluorescent nanomaterials may constitute the basis of new strategies in the development of methods for the detection of CEA. QDs, such as core/shell CdSe/ZnS, also referred to as semiconductor nanocrystals, show high fluorescence efficiency, robustness, and flexibility of functionalization towards conjugating ligands for selective nano-sensing of analytes [35–40]. Thus, expanding the applications of QDs to develop sensitive and simple sensors for the detection of various analytes is a topic of current interest [41–43].

Although QDs encapsulated in microparticles possess qualified fluorescence [39, 44], the encapsulation is time-consuming and aggregation would be a significant problem during short-term storage. Therefore, investigations into water-soluble QDs have been widely reported. However, these are normally applied in bio-imaging rather than homogeneous fluoroassays, so there have been no commercial products developed to date for research or clinical diagnosis. Consequently, there are few reports regarding the use of the pairs of combined QDs and luminescent lanthanide complexes for homogenous immunoassays [42, 45, 46].

In the current research, luminescent terbium chelates (LTCs) and QDs were synthesized and used as an energy donor and acceptor, respectively, with the fluorescence of QDs time-resolved and named after time-resolved Förster resonance transfer (TR-FRET). The energy donor and the acceptor were each conjugated with a different anti-CEA monoclonal antibody (McAb). Using the double-antibodies sandwich mode, the TR-FRET was thereby sensitized and used to detect standard samples of CEA in 96-wells plates. Our results are expected to extend the applications of QD nanoparticles in homogeneous clinical bioassays in the future.

Materials and Methods

Tri-n-octylphosphine oxide (TOPO), tri-n-octylphosphine, bis(trimethylsilyl)sulfide ($(TMS)_2S$), 2-[N-morpholino] ethanesulfonic acid (MES), diethylenetriaminepentaacetic acid (DTPA), diethylenetriaminepentaacetic acid dianhydride (DTPAa), 7-amino-4-methyl-2(*1H*)-quinolinone (cs124), ethylenediamine (EDA), $TbCl_3$•$6H_2O$, and anhydrous dimethyl sulfoxide (DMSO) were purchased from Sigma–Aldrich Fine Chemicals (St. Louis, MO). Cadmium acetate ($Cd(Ac)_2$), zinc acetate ($Zn(Ac)_2$), selenium, tetramethylammonium hydroxide, hexadecylamine, were purchased from Acros Organics(Geel, Belgium). All economical synthetic routes for CdSe/ZnS core/shell QDs were carried out under argon using the Schlenk technique in a glovebox. Samples involved were centrifuged at 14,000 g for 10 mins.

Monoclonal anti-CEA McAbs produced in mice (clone codes 6 F11 and S001) and CEA standards were purchased from Medix (Grankulla, Finland). Bis(sulfosuccinimidyl) suberate sodium salt (BS3), glutathione reduced (GSH), ethylenediaminetetraacetic acid (EDTA), (N-(3-dimethyllaminopropyl) carbodiimide hydrochloride (EDAC), Tris(hydroxymethyl) aminomethane (Tris), and N-hydroxysulfosuccinimide sodium salt (Sulfo-NHS) were purchased from Thermo Fisher Scientific Inc. All other chemicals used were of analytical grade.

Preparation of Water-Soluble QDs

TOPO-capped shell/core ZnS/CdSe QDs in chloroform at 8 μM were prepared in our previous reports [44, 47, 48]. GSH-capped QDs were prepared by replacing the TOPO using previously described methods [35, 48, 49] with a range of modifications from TOPO-capped QDs, described briefly as follows: 50 μl of QDs was added to 15 mg GSH by vigorous shaking. After 4 h, solutions of NaOH (1 M, 10 μl), chloroform (10 μl) and acetone (1 ml) were added successively and mixed thoroughly. The mixture was centrifuged and the precipitate was collected and dissolved in deionized water (50 μl). The QDs solution was washed by adding 1 ml of acetone and centrifuging, after which the precipitate was collected. The washing step was repeated at least four times. Finally, the QDs were dissolved in MES buffer (0.5 M, 0.5 ml).

Conjugation of QDs with Anti-CEA Monoclonal Antibodies

To avoid bridging of the particles by covalently coupled protein and cross-linking of the protein, a two-step procedure is often preferred. 1 ml of a mixture of QDs (8 μM), MES buffer (0.5 M, 0.1 mL), sulfo-NHS (250 mM, 0.23 mL) and EDAC (100 mM, 0.23 mL) was incubated for 30 min at room temperature with stirring. Then the mixture was centrifuged with a Microcon YM-50 Centrifugal Filter Unit (Millipore) and washed three times with MES buffer. The QDs were resuspended at a final concentration of 1 mg/mL in phosphate buffered saline (PBS, 50 mM, pH7.4). 100 μL of McAbs 6 F11 (1 mg/mL) in PBS was added with stirring. The final concentrations of proteins in the conjugates mixture were 1 mg/mL. The mixture was incubated with gentle mixing for 2.5 h and then 2.5 μL of ethanolamine was added and incubated for another 30 min with gentle stirring. The unbound protein and ethanolamine were then removed with a Microcon YM-50 Centrifugal Filter Unit and washed with buffer containing 25 mM Tris–HCl, 0.15 M NaCl, 0.05 % Tween 20, pH7.2. The resultant product (QDs-6 F11) was stored with a McAbs concentration of 0.1 mg/mL at 4 °C in PBS with 0.01 % sodium azide for the subsequent detection.

Synthesis of LTCs

The chelators of LTCs were cs124-DTPA-EDA in anhydrous DMSO with DTPAa, cs124 and EDA, purified by high performance liquid chromatography as previously reported [32, 33, 50]. The cs124-DTPA-EDA was added at a 1:1.1 molar ratio to a solution of $TbCl_3$•$6H_2O$ in triethylammonium acetate, pH5. The solution was then incubated at room temperature for 1 h, after which the solution was monitored by the fluorescence spectrometer and EDTA solution (5 μM) added slowly until the intensity of the time-resolved fluorescence began to decrease. The product of LTCs was diluted to 42 μg/mL in PBS buffer and kept at 4 °C for the subsequent conjugation.

Determination of Quantum Yields of QDs and LTCs

The fluorescence and absorption spectra of QDs with 565 nm emission and LTCs were collected on a LS-55 Fluorescence Spectrometer (PerkinElmer Inc., Waltham, MA) and UV–vis spectrophotometer (UV-2550, Shimadzu, Japan), respectively.

The quantum yield of QDs was actually obtained referencing Rhodamine 6 G, for which the QY is known to be 95 %, according to the literature [35, 36, 48, 51]. The quantum yield of LTCs was determined [52–54] by using a standard solution of 0.1 μM Eu^{3+} in *Wallac Delfia* enhancement solution. Note that the optical density was below 0.1 at the first absorption peak of the QDs, and that the fluorescence of LTCs was corrected for the photomultiplier quantum-yield difference (1.39-fold at 545 nm compared with the value at 613 nm).

Conjugation of LTCs with Anti-CEA McAbs

100 μL of the prepared LTCs (8 μM) was added to 100 μL of McAbs S001 (1 mg/mL) and stirred thoroughly. The

mixture was added to BS3 with excess LTCs, and incubated at room temperature for 1 h with gentle shaking. After incubation, the mixture was centrifuged with a Microcon YM-50 Centrifugal Filter Unit (Millipore) and washed five times with PBS. The LTC-S001 product was collected and diluted to a McAbs concentration of 0.1 mg/mL with 0.01 % sodium azide.

Preparation of Antigen Standards

The CEA antigen was diluted into six standard samples (0, 1, 5, 10, 100, 200 ng/mL) using 50 mM Tris–HCl buffer containing 1.5 % BSA and 0.15 % NaN_3, with the help of Daan Gene Co., Ltd. of Sun Yat-sen University. All concentrations of samples were verified using a NanoDrop 2000 (Thermo Fisher Scientific Inc.) and stored at 4 °C.

Detection of CEA Using LTCs and QDs

HTRFA for CEA was carried out using the double-antibodies sandwich-type immunoassay in a one-step assay procedure. In brief, the standards (25 μL) were added to 96-well plates and then 50 μL of the assay buffer containing LTC-S001 and 50 μL of QDs-6 F11 in assay buffer was added. The plates were covered and incubated at 37 °C for 45 min. Under the time-resolved fluorescence mode, the samples were measured with a 565 nm emission filter (bandwidth 10 nm) on a Victor^3 V 1420 Multilabel Plate Reader (PerkinElmer Wallac, Turku, Finland). The TR-FRET signals were collected from the transparent bottom of the plate with 340 nm excitation and 565 nm emission (Delay time 100 μs; window time 100 μs; circle 3000).

Results and Discussion

Synthesis and Characterization of QDs and LTCs

To obtain the QDs at a high quantum yield, the most popular methods are to prepare them in an organic phase [36, 38, 48, 55] or to incorporate them into microparticles [37, 39]. Although microparticles containing QDs have many advantages, aggregation during storage and application is problematic. Meanwhile, GSH-capped QDs also offer many advantages. Their preparation is relatively simple and can retain most of the photo-properties of oil-soluble QDs, except at a lower quantum yield (QY), as shown in Fig. 1 and Table 1. The quantum yield (Φ) can be expressed by Eq. (1) as:

$$\Phi = \Phi_r \cdot \frac{I_{int}}{I_{int,r}} \frac{A_r}{A} \frac{n^2}{n_r^2}, \quad (1)$$

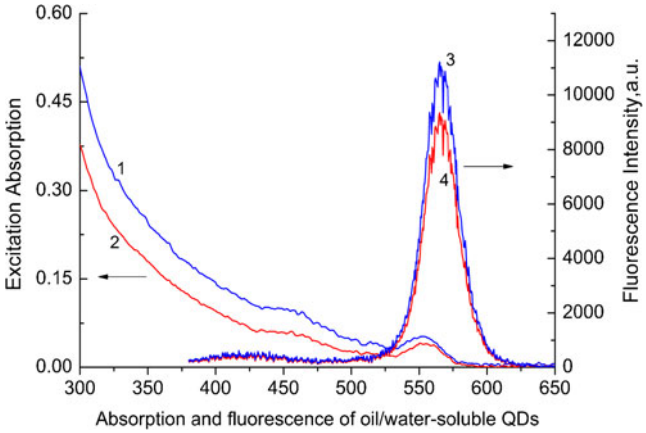

Fig. 1 Absorption and fluorescence spectra of TOPO-capped QDs in chloroform and GSH-capped QDs in water. The blue curves (1 and 3) are the absorption and fluorescence spectra of TOPO-capped QDs and the red curves (2 and 4) are those of GSH-capped QDs

where Φ or Φ_r is the quantum yield of water or oil-soluble QDs, I_{int} or $I_{int,r}$ is the area under the emission peak of water or oil-soluble QDs over 350–650 nm with 350 nm excitation; A or A_r is the absorbance at the excitation wavelength (350 nm), and n or n_r are the refractive index of the water (1.333) and n-hexane (1.375), respectively.

According to Eq. (1) and Fig. 1, one can see that Φ of water-soluble QDs (wQDs) was 90.3 % that of Φ_r for oil-soluble QDs (oQDs). The full-width at half maximum (FWHM) of oQDs remained at 28.5 nm. Such a narrow FWHM is very important for multiple bioanalyses. On the contrary, the FWHM of QDs encapsulated in microparticles or prepared indirectly from a water-phase is always much broader than that for oQDs [37, 39]. Because different protocols were used, the FWHM of GSH-QDs was narrower than for those prepared directly from the water-phase.

However, the total shell of GSH-capped QDs is so thin that it is more suitable for FRET applications than those encapsulated within microparticles [56]. Furthermore, the bifunctional groups ($-NH_2$, -COOH) of GSH were very important during storage to keep QDs in the hydrogel state. In our case, GSH-capped QDs could be kept for more than 6 months without aggregation. Therefore, similar to many other researchers [36, 38], we used these as fluorophores to label antibodies for the double-antibody sandwich immunoassay in this study. However, QDs doped in polystyrene microparticles (QPs) caused aggregation in practice [39, 44]. It is difficult to obtain stable and efficient QPs, whereas the QDs retained a high quality. Considering the distance-dependence of FRET, water-soluble QDs are an ideal type of fluorophore for biomolecular analysis. The versatility of GSH-capped QDs has been verified by many researchers [55]. In such work, QDs were capped by GSH with reduced amino and carboxyl groups, which could be conjugated to proteins at high quantum yield [57]. In our case, the

Table 1 Comparison of the physical properties of TOPO-capped QDs in chloroform and GSH-capped QDs in water

Items	Ligand	Solution	Size, nm[a]	FWHM, nm	Absorption Peak, nm	Emission Peak, nm	Conc., mol/L[a]	QY, %
oQDs	TOPO	n-hexane	3.1	28.5	553.0	565.0	4.5×10^{-7}	Φ
wQDs	GSH	water	3.1	28.5	552.5	565.0	3.3×10^{-7}	0.903Φ

[a] Calculated according to Ref. 46

quantum yield of GSH-capped QDs was around 40 %. The amino groups of GSH on the surface of QDs were coupled with the amino groups on the antibodies forming QDs-6 F11 conjugates. In the absence of the outer shell of doping materials, GSH-QDs were used as the energy acceptor in the TR-FRET immunoassay (Fig. 2).

LTCs were prepared as previously [50] and their structure is shown in Fig. 2. The terbium ions chelated with cs124-DTPA. Cs124 worked as an antenna, which made terbium ions luminescent because of inner-FRET. The cs124 antenna transferred energy to terbium ions in the LTC molecule. The fluorescence of LTCs possessed an extended lifetime and was time-solved with about 65 % quantum yield, suitable for FRET analysis [32, 33]. The primary amino group on EDA of the LTC was conjugated with the carboxyl group of the monoclonal antibody to form stable covalently bonded conjugates (LTCs-S001).

Detection of CEA Standard Samples Using LTC-S001 and QDs-6 F11

There are a small number of reports describing the combination of QDs-LTCs pairs used for TR-FRET-based homogeneous immunoassays [42, 56]. To enhance the FRET efficiency, the key issue is to enhance the Förster distance (R_0). Researchers have made efforts on the qualified fluorescence of energy acceptors (QDs) and donors (LTCs). Therefore, QDs-doping and preparation of LTCs with high quantum yield are hot topics in TR-FRET study. It is well known that doping-QDs possess essential disadvantages (thicker shells and aggregation). Anthor, the commercial LTC possessing the highest QY, is a tribipyridin chelator, which is patent-protected and very expensive. Therefore, the practical approach is to make QDs with high efficiency and thin shells, and then pair them with available LTCs for TR-FRET.

In this paper, the synthesized QDs were not made from polymer or microparticles but from GSH. LTCs with a very simple molecular structure were used (Fig. 2) and the protocol involved was facile. These were then used for detecting the CEA samples by TR-FRET. With LTCs-S001 McAbs serving as energy donors, QDs-6 F11 McAbs were then applied in the homogeneous immunoassay as energy acceptors, as shown.

It is important to consider the Förster distance (R_0) in the FRET-based homogenous assay using LTCs and QDs. The

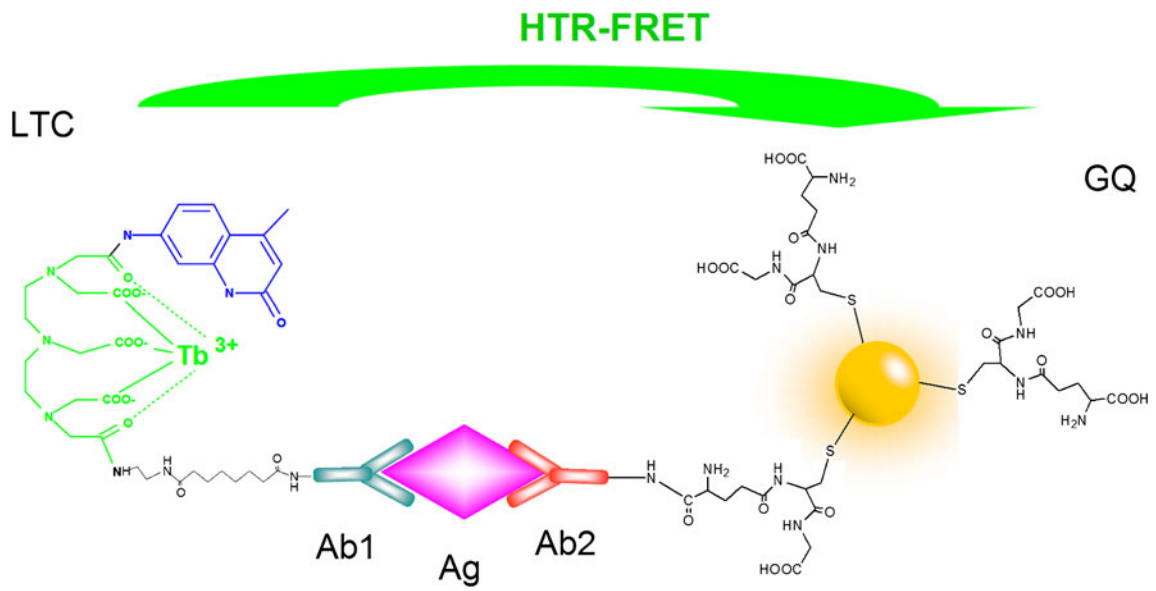

Fig. 2 Principle of LTCs and QDs-based homogeneous time-resolved fluoroimmunoassay with LTCs conjugates. Ab1, Ab2, Ag and GQ refer to McAb 6 F11, McAbS001, CEA and GSH-capped QDs, respectively

Förster distance involves components from the spectral properties and is expressed as follows [58–60]:

$$R_0^6 = \frac{9000(\ln 10)\kappa^2 Q_D}{128\pi^5 N_A n^4} \int_0^\infty F_D(\lambda)\varepsilon_A(\lambda)\lambda^4 d\lambda, \quad (2)$$

where Q_D is the quantum yield of the donor in the absence of an acceptor; n is the refractive index of the medium; n^2 is a factor describing the relative orientation in space of the transition dipoles of the donor and acceptor, which is usually assumed to be equal to 2/3; N_A is the Avogadro constant; r is the distance between the donor and acceptor; $F_D(\lambda)$ is the corrected fluorescence intensity of the donor in the wavelength range λ to $\lambda+\Delta\lambda$ with the total intensity normalized to unity; and $\varepsilon(\lambda)$ is the extinction coefficient of the acceptor at λ.

$J(\lambda)$ is the overlap integral of the involved spectra of donors and accepters[60]:

$$J(\lambda) = \int_0^\infty F_D(\lambda)\varepsilon_A(\lambda)\lambda^4 d\lambda = \frac{\int_0^\infty F_D(\lambda)\varepsilon_A(\lambda)\lambda^4 d\lambda}{\int_0^\infty F_D(\lambda) d\lambda}. \quad (3)$$

This expresses the degree of spectral overlap between the donor emission and the acceptor absorption. In our investigation, the donor was LTC (conjugated with S001 McAbs) and the acceptor was QDs (conjugated with 6 F11 McAbs). The absorption spectra of QDs and time-resolved fluorescence spectra of LTCs are shown in Fig. 3. Expressing the wavelength in nm, one could find from Fig. 3

$$J(\lambda) = 6.77 \times 10^{15} M^{-1} cm^{-1} nm^4,$$

and the Förster distance[60] in Å can be given by:

$$R_0 = 0.211\left(\kappa^2 n^{-4} Q_D J(\lambda)\right)^{1/6}, \quad (4)$$

where Q_D is the quantum yield of LTCs-S001, 67 %, and R_0 was calculated as 61.9 Å, which was shorter than the Förster distance (10 nm). Therefore, TR-FRET could be sensitized in theory, between LTCs-S001 and QDs-6 F11.

The efficiency (η) of TR-FRET can be expressed as[60]:

$$\eta_{FRET} = \frac{R_0^6}{R_0^6 + r^6}, \quad (5)$$

where, r is the donor-acceptor distance. From Eq. (5), one can see that the surface of QDs plays a very important role in TR-FRET. If encapsulated within microparticles, the distance (r) between QDs and LTCs would definitely be greatly increased. Therefore, it is necessary to synthesize GSH-QDs from oil-soluble QDs.

Because of the short lifetime of QDs, their fluorescence can be neglected in time-resolved mode. When collecting data, there are always some interfering factors from the decay in fluorescence of QDs, the laser source and background signal (auto-fluorescence). It is very important to avoid auto-fluorescence. In our case, the decay in auto-fluorescence was examined with the QDs solution (in the absence of LTCs), shown in Fig. 4. One can see that when the delay time was longer than 100 μs, the signal from auto-fluorescence could be neglected. This is to say, once the fluorescence signals were detected at 565 nm, the TR-FRET would be triggered and the signals left after subtracting those from LTCs at 565 nm must be the fluorescence emitted from the QDs. Therefore, the delay time in the time-resolved mode was optimized using Fig. 4. for the detection of CEA standard samples using LTC-S001 and QDs-6 F11.

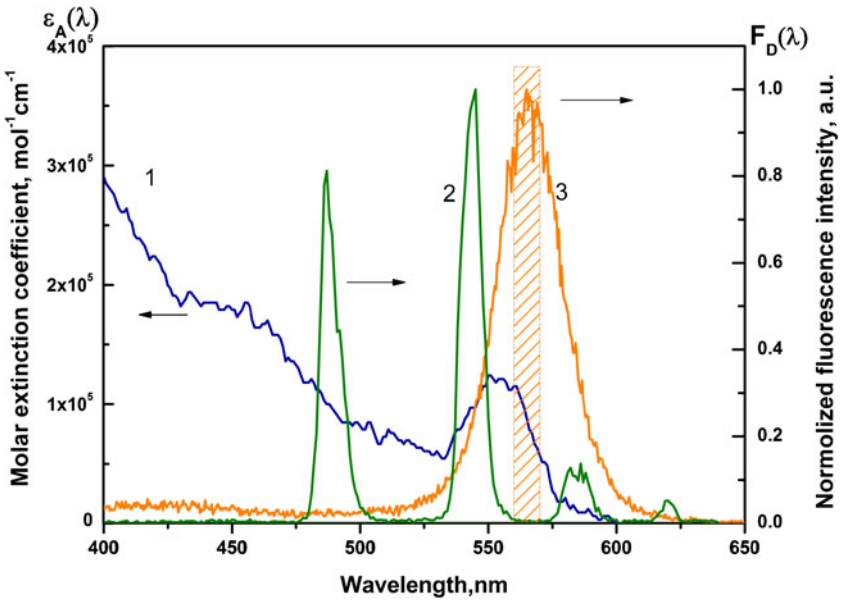

Fig. 3 Spectral overlap of LTCs and QDs-based homogeneous time-resolved fluoroimmunoassay. The blue curve (1) on the left is the absorption spectrum of QDs. The green curve (2) on the right is the time-resolved fluorescence spectrum of LTCs. The orange curve (3) on the right is the normalized fluorescence spectrum of QDs. The rectangle with a sparse pattern is the model of the emission filter with a 10 nm bandwidth

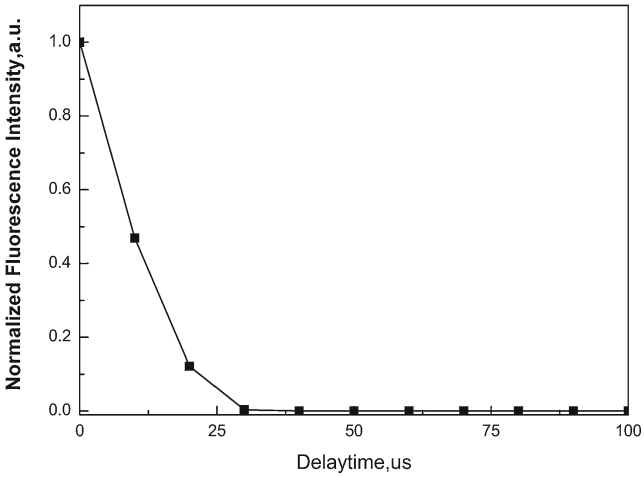

Fig. 4 Option of delay time of detection based on the luminescence decay of energy acceptors (QDs)

In the double-antibodies sandwich mode, the QDs-6 F11 and LTCs-S001 were in excess and an immunocomplex was formed, which made the energy acceptors (QDs) and donors (LTCs) approach one another. As a result, the TR-FRET was sensitized and QDs emitted time-resolved fluorescence [61], which was magnified many times in time-resolved mode. Therefore, the fluorescence intensity at the emission peak of QDs (565 nm) was detected and was positively proportional to the amount of CEA, as shown in Fig. 5. The standard curve was obtained using the following fitted equation: LogY=2.75566+0.94457 LogX (R=0.998, where X and Y are the concentrations of CEA and the fluorescence intensity at 565 nm, respectively). The analytical sensitivity (dose of mean zero plus 2 SD) was calculated by 0.4 ng/mL. This meant the developed method gave a good linear dynamic range in our investigation. Therefore, the results indicated that GSH-QDs without encapsulation in microparticles possessed a thinner shell and this shortened the distance between energy donors and acceptors. The shorter distance was necessary for TR-FRET and could be used to detect the cancer marker.

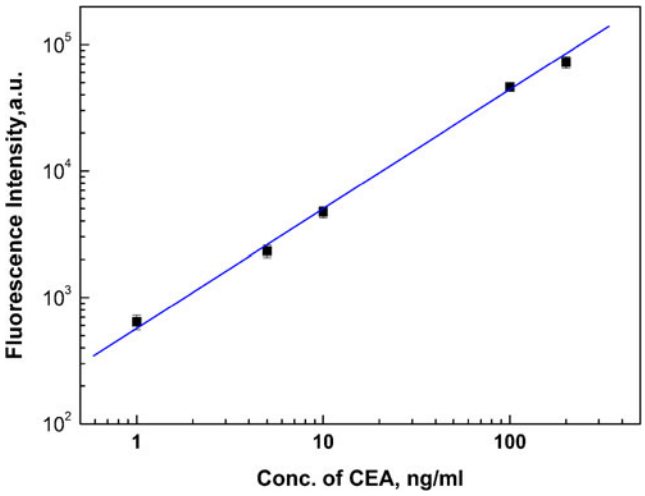

Fig. 5 Standard curve of the LTCs and QDs-based homogeneous time-resolved fluoroimmunoassay for detection of CEA. The fitting line is LogY=2.75566+0.94457 LogX (R=0.998). The triangles were plotted according to the fluorescence intensity of the test samples with the standard curve

Conclusions

In conclusion, water-soluble QDs with GSH and luminescent terbium chelates were both prepared. These were then conjugated with anti-CEA McAbs to prepare QDs-6 F11 and LTCs-S001, respectively. QDs-6 F11 and LTCs-S001 were used as an energy acceptor and donor, respectively in the detection of CEA. Resonance energy transfer took place and QDs fluorescence was detected as positive signals in time-resolved mode. The results indicate that water-soluble QDs were suitable for the homogeneous immunoassay. This work will extend the applications of QDs in homogeneous clinical bioassays for cancer markers in the future. The photo-properties of prepared GSH-capped QDs were suitable for homogeneous multiplex immunoassays, which require high throughput or the consideration of multiple factors in cancer screening.

Acknowledgements The work was supported by the National Natural Science Foundation of China (Grant No. 30901382, 81271931), the Natural Science Foundation of Guangdong Province (No. S2012010009547), the New Teacher for Doctoral Fund of Ministry of Education of China (Grant No. 20094433120008), Special Funds for College and University Talents by Guangdong Province (2009) and Scientific Research Foundation of Introducing Talents of Southern Medical University(2009).

Competing interests None.

Funding The National Natural Science Foundation of China (Grant No. 30901382, 81271931), the New Teacher for Doctoral Fund of Ministry of Education of China (Grant No. 20094433120008), the Natural Science Foundation of Guangdong Province (No. S2012010009547), Special Funds for College and University Talents by Guangdong Province (2009), and the Scientific Research Foundation of Introducing Talents of Southern Medical University(2009).

Ethical approval The Ethical Committee of Science and Technology Department of Southern Medical University approved this study (REC number: 20121058B).

Guarantor Tian-Cai Liu.

Contributorship Mei-Jun Chen, Jing-Yuan Hou and Da Sun contributed to experimental work. Tian-Cai Liu and Ying-Song Wu researched literature and conceived the study. Mei-Jun Chen and Zhi-Qi Ren were involved in protocol development, gaining ethical approval, and data analysis. Mei-Jun Chen wrote the first draft of the manuscript. All authors reviewed and edited the manuscript and approved the final version of the manuscript.

References

1. Gold P, Freedman SO (1965) Demonstration of tumor-specific antigens in human colonic carcinomata by immunological tolerance and absorption techniques. J Exp Med 121:439–462
2. Gold P, Freedman SO (1965) Specific carcinoembryonic antigens of the human digestive system. J Exp Med 122(3):467–481
3. Tsai HL, Chang YT, Chu KS, Chen CF, Yeh YS, Ma CJ, Wu DC, Kuo CH, Chan HM, Sheen MC, Wang JY (2008) Carcinoembryonic antigen in monitoring of response to cetuximab plus FOLFIRI or FOLFOX-4 in patients with metastatic colorectal cancer. Int J Biol Markers 23(4):244–248
4. Duxbury MS, Ito H, Benoit E, Waseem T, Ashley SW, Whang EE (2004) A novel role for carcinoembryonic antigen-related cell adhesion molecule 6 as a determinant of gemcitabine chemoresistance in pancreatic adenocarcinoma cells. Cancer Res 64(11):3987–3993. doi:10.1158/0008-5472.CAN-04-0424
5. Tanaka T, Huang J, Hirai S, Kuroki M, Watanabe N, Tomihara K, Kato K, Hamada H (2006) Carcinoembryonic antigen-targeted selective gene therapy for gastric cancer through FZ33 fiber-modified adenovirus vectors. Clin Cancer Res 12(12):3803–3813. doi:10.1158/1078-0432.CCR-06-0024
6. Yoon SM, Shin KH, Kim JY, Seo SS, Park SY, Kang S, Cho KH (2007) The clinical values of squamous cell carcinoma antigen and carcinoembryonic antigen in patients with cervical cancer treated with concurrent chemoradiotherapy. Int J Gynecol Cancer 17(4):872–878. doi:10.1111/j.1525-1438.2007.00878.x
7. Chu TM, Reynoso G, Hansen HJ (1972) Demonstration of carcinoembryonic antigen in normal human plasma. Nature 238(5360):152–153
8. Withofs M, Offner F, de Paepe P, Praet M (2000) Carcinoembryonic antigen elevation in agnogenic myeloid metaplasia. Br J Haematol 110(3):743–744
9. Kodera Y, Isobe K, Yamauchi M, Satta T, Hasegawa T, Oikawa S, Kondoh K, Akiyama S, Itoh K, Nakashima I et al (1993) Expression of carcinoembryonic antigen (CEA) and nonspecific crossreacting antigen (NCA) in gastrointestinal cancer; the correlation with degree of differentiation. Br J Cancer 68(1):130–136
10. Shousha S, Lyssiotis T, Godfrey VM, Scheuer PJ (1979) Carcinoembryonic antigen in breast-cancer tissue: a useful prognostic indicator. Br Med J 1(6166):777–779
11. Ishiguro F, Fukui T, Mori S, Katayama T, Sakakura N, Hatooka S, Mitsudomi T (2010) Serum carcinoembryonic antigen level as a surrogate marker for the evaluation of tumor response to chemotherapy in nonsmall cell lung cancer. Ann Thorac Cardiovasc Surg 16(4):242–247
12. Hsu WH, Huang CS, Hsu HS, Huang WJ, Lee HC, Huang BS, Huang MH (2007) Preoperative serum carcinoembryonic antigen level is a prognostic factor in women with early non-small-cell lung cancer. Ann Thorac Surg 83(2):419–424. doi:10.1016/j.athoracsur.2006.07.079
13. de Diego A, Compte L, Sanchis J, Enguidanos MJ, Marco V (1991) Usefulness of carcinoembryonic antigen determination in bronchoalveolar lavage fluid. A comparative study among patients with peripheral lung cancer, pneumonia, and healthy individuals. Chest 100(4):1060–1063
14. van Nagell JR Jr, Donaldson ES, Wood EG, Goldenberg DM (1978) The clinical significance of carcinoembryonic antigen in the plasma and tumors of patients with gynecologic malignancies. Cancer 42(3 Suppl):1527–1532
15. Shibata S, Raubitschek A, Leong L, Koczywas M, Williams L, Zhan J, Wong JY (2009) A phase I study of a combination of yttrium-90-labeled anti-carcinoembryonic antigen (CEA) antibody and gemcitabine in patients with CEA-producing advanced malignancies. Clin Cancer Res 15(8):2935–2941. doi:10.1158/1078-0432.CCR-08-2213
16. Maziak W (2008) Carcinoembryonic antigen (CEA) levels in hookah smokers, cigarette smokers and non-smokers–a comment. J Pak Med Assoc 58(3):155
17. Stevens DP, Mackay IR (1973) Increased carcinoembryonic antigen in heavy cigarette smokers. Lancet 2(7840):1238–1239
18. Urva SR, Yang VC, Balthasar JP (2009) Development and validation of an enzyme linked immunosorbent assay for the quantification of carcinoembryonic antigen in mouse plasma. J Immunoass Immunochem 30(4):418–427. doi:10.1080/15321810903188227
19. Franchimont P, Debruche ML, Zangerlee PF, Proyard J (1973) Radioimmunoassay of the carcinoembryonic antigen. Ann Immunol (Paris) 124(4):619–630
20. Tsaltas G, Ford CH, Gallant M (1992) Demonstration of monoclonal anti-carcinoembryonic antigen (CEA) antibody internalization by electron microscopy, western blotting and radioimmunoassay. Anticancer Res 12(6B):2133–2142
21. Hou JY, Liu TC, Lin GF, Li ZX, Zou LP, Li M, Wu YS (2012) Development of an immunomagnetic bead-based time-resolved fluorescence immunoassay for rapid determination of levels of carcinoembryonic antigen in human serum. Anal Chim Acta 734(93):93–98. doi:10.1016/j.aca.2012.04.044
22. Stockley RA, Shaw J, Whitfield AG, Whitehead TP, Clarke CA, Burnett D (1986) Effect of cigarette smoking, pulmonary inflammation, and lung disease on concentrations of carcinoembryonic antigen in serum and secretions. Thorax 41(1):17–24
23. Sajid KM, Chaouachi K, Mahmood R (2008) Hookah smoking and cancer: carcinoembryonic antigen (CEA) levels in exclusive/ever hookah smokers. Harm Reduct J 5:19. doi:10.1186/1477-7517-5-19
24. Dungchai W, Siangproh W, Lin JM, Chailapakul O, Lin S, Ying X (2007) Development of a sensitive micro-magnetic chemiluminescence enzyme immunoassay for the determination of carcinoembryonic antigen. Anal Bioanal Chem 387(6):1965–1971. doi:10.1007/s00216-006-0899-y
25. Yang X, Guo Y, Wang A (2010) Luminol/antibody labeled gold nanoparticles for chemiluminescence immunoassay of carcinoembryonic antigen. Anal Chim Acta 666(1–2):91–96. doi:10.1016/j.aca.2010.03.059
26. Matsushita H, Xu J, Kuroki M, Kondo A, Inoue E, Teramura Y, Nozawa M, Senba T, Yamamoto T, Matsuoka Y (1996) Establishment and evaluation of a new chemiluminescent enzyme immunoassay for carcinoembryonic antigen adapted to the fully automated ACCESS system. Eur J Clin Chem Clin Biochem 34(10):829–835
27. Haggart R, Thorpe GH, Moseley SB, Kricka LJ, Whitehead TP (1986) An enhanced chemiluminescent enzyme immunoassay for serum carcinoembryonic antigen based on a modification of a commercial kit. J Biolumin Chemilumin 1(1):29–34. doi:10.1002/bio.1170010106
28. Kricka LJ (1994) Selected strategies for improving sensitivity and reliability of immunoassays. Clin Chem 40(3):347–357
29. Dickson EF, Pollak A, Diamandis EP (1995) Ultrasensitive bioanalytical assays using time-resolved fluorescence detection. Pharmacol Ther 66(2):207–235
30. Blomberg KR, Mukkala VM, Hakala HH, Makinen PH, Suonpaa MU, Hemmila IA (2011) A dissociative fluorescence enhancement technique for one-step time-resolved immunoassays. Anal Bioanal Chem 399(4):1677–1682. doi:10.1007/s00216-010-4485-y
31. Mathis G, Socquet F, Viguier M, Darbouret B (1997) Homogeneous immunoassays using rare earth cryptates and time resolved fluorescence: principles and specific advantages for tumor markers. Anticancer Res 17(4B):3011–3014
32. Selvin PR, Hearst JE (1994) Luminescence energy transfer using a terbium chelate: improvements on fluorescence energy transfer. Proc Natl Acad Sci U S A 91(21):10024–10028

33. Li M, Selvin PR (1997) Amine-reactive forms of a luminescent diethylenetriaminepentaacetic acid chelate of terbium and europium: attachment to DNA and energy transfer measurements. Bioconjug Chem 8(2):127–132. doi:10.1021/bc960085m
34. Leyris JP, Roux T, Trinquet E, Verdie P, Fehrentz JA, Oueslati N, Douzon S, Bourrier E, Lamarque L, Gagne D, Galleyrand JC, M'Kadmi C, Martinez J, Mary S, Baneres JL, Marie J (2011) Homogeneous time-resolved fluorescence-based assay to screen for ligands targeting the growth hormone secretagogue receptor type 1a. Anal Biochem 408(2):253–262. doi:10.1016/j.ab.2010.09.030
35. Bruchez M Jr, Moronne M, Gin P, Weiss S, Alivisatos AP (1998) Semiconductor nanocrystals as fluorescent biological labels. Science 281(5385):2013–2016
36. Chan WC, Nie S (1998) Quantum dot bioconjugates for ultrasensitive nonisotopic detection. Science 281(5385):2016–2018
37. Gerion D, Pinaud F, Williams SC, Parak WJ, Zanchet D, Weiss S, Alivisatos AP (2001) Synthesis and properties of biocompatible water-soluble silica-coated CdSe/ZnS semiconductor quantum dots. J Phys Chem B 105(37):8861–8871. doi:10.1021/jp0105488
38. Chan WC, Maxwell DJ, Gao X, Bailey RE, Han M, Nie S (2002) Luminescent quantum dots for multiplexed biological detection and imaging. Curr Opin Biotechnol 13(1):40–46
39. Han M, Gao X, Su JZ, Nie S (2001) Quantum-dot-tagged microbeads for multiplexed optical coding of biomolecules. Nat Biotechnol 19(7):631–635. doi:10.1038/9022890228
40. Law WC, Yong KT, Roy I, Ding H, Hu R, Zhao W, Prasad PN (2009) Aqueous-phase synthesis of highly luminescent CdTe/ZnTe core/shell quantum dots optimized for targeted bioimaging. Small 5(11):1302–1310. doi:10.1002/smll.200801555
41. Algarra M, Campos BB, Miranda MS, da Silva JC (2011) CdSe quantum dots capped PAMAM dendrimer nanocomposites for sensing nitroaromatic compounds. Talanta 83(5):1335–1340. doi:10.1016/j.talanta.2010.10.056
42. Charbonniere LJ, Hildebrandt N, Ziessel RF, Lohmannsroben HG (2006) Lanthanides to quantum dots resonance energy transfer in time-resolved fluoro-immunoassays and luminescence microscopy. J Am Chem Soc 128(39):12800–12809. doi:10.1021/ja062693a
43. Azzazy HM, Mansour MM, Kazmierczak SC (2006) Nanodiagnostics: a new frontier for clinical laboratory medicine. Clin Chem 52(7):1238–1246. doi:10.1373/clinchem.2006.066654
44. Wang HQ, Huang ZL, Liu TC, Wang JH, Cao YC, Hua XF, Li XQ, Zhao YD (2007) A feasible and quantitative encoding method for microbeads with multicolor quantum dots. J Fluoresc 17(2):133–138. doi:10.1007/s10895-007-0157-5
45. Morgner F, Stufler S, Geissler D, Medintz IL, Algar WR, Susumu K, Stewart MH, Blanco-Canosa JB, Dawson PE, Hildebrandt N (2011) Terbium to quantum Dot FRET bioconjugates for clinical diagnostics: influence of human plasma on optical and assembly properties. Sensors (Basel) 11(10):9667–9684. doi:10.3390/s111009667
46. Charbonnière LJ, Hildebrandt N (2008) Lanthanide complexes and quantum dots: a bright wedding for resonance energy transfer. European Jounal of Inorganic Chmistry 2008(21):3241–3251. doi:10.1002/ejic.200800332
47. Yu WW, Qu L, Guo W, Peng X (2003) Experimental determination of the extinction coefficient of CdTe, CdSe, and CdS nanocrystals. Chem Mater 15(14):2854–2860. doi:10.1021/cm034081k
48. Liu TC, Huang ZL, Wang HQ, Wang JH, Li XQ, Zhao YD, Luo QM (2006) Temperature-dependent photoluminescence of water-soluble quantum dots for a bioprobe. Anal Chim Acta 559(1):120–123. doi:10.1016/j.aca.2005.11.053
49. Freeman R, Liu X, Willner I (2011) Amplified multiplexed analysis of DNA by the exonuclease III-catalyzed regeneration of the target DNA in the presence of functionalized semiconductor quantum dots. Nano Lett 11(10):4456–4461. doi:10.1021/nl202761g
50. Dong ZN, Wu YS, Wang Z, He A, Li M, Chen M, Du H, Ma Q, Liu T (2012) Effect of temperature on the photoproperties of luminescent terbium sensors for homogeneous bioassays. Luminescence. doi:10.1002/bio.2355
51. Kubinm RF, Fletcher AN (1982) Fluorescence quantum yields of some rhodamine dyes. J Luminescence 27:455–462
52. Hemmilä IA, Mikola HJ (1990) New complexing agents for labeling of proteins with metals. Acta Radiol Suppl 374:53–55
53. Hemmilä I, Mukkala V-M, Takalo H (1997) Development of luminescent lanthanide chelate labels for diagnostic assays. J Alloys Comp 249(1–2):158–162. doi:10.1016/S0925-8388(96)02834-4
54. Hemmilä I, Dakubu S, Mukkala V-M, Siitari H, Lövgren T (1984) Europium as a label in time-resolved immunofluorometric assays. Anal Biochem 137(2):335–343
55. Wang J, Jiang P, Han Z, Qiu L, Wang C, Zheng B, Xia J (2012) Fast self-assembly kinetics of quantum dots and a dendrimeric peptide ligand. Langmuir 28(21):7962–7966. doi:10.1021/la301227r
56. Hildebrandt N, Geissler D (2012) Semiconductor quantum dots as FRET acceptors for multiplexed diagnostics and molecular ruler application. Adv Exp Med Biol 733:75–86. doi:10.1007/978-94-007-2555-3_8
57. Perez-Donoso JM, Monras JP, Bravo D, Aguirre A, Quest AF, Osorio-Roman IO, Aroca RF, Chasteen TG, Vasquez CC (2012) Biomimetic, mild chemical synthesis of CdTe-GSH quantum dots with improved biocompatibility. PLoS One 7(1):e30741. doi:10.1371/journal.pone.0030741
58. Schulman SG (1977) Fluorescence and phosphorescence spectroscopy: physicochemical principles and practice. Pergamon, Oxford
59. Valeur B (2002) Molecular fluorescence: principles and applications. Wiley-VCH, Weinheim; Chichester
60. Lakowicz JR (1999) Principles of fluorescence spectroscopy, 2nd edn. Kluwer Academic/Plenum, New York; London
61. Morgner F, Geissler D, Stufler S, Butlin NG, Lohmannsroben HG, Hildebrandt N (2010) A quantum-dot-based molecular ruler for multiplexed optical analysis. Angew Chem Int Ed Engl 49(41):7570–7574. doi:10.1002/anie.201002943